Heliyon 6 (2020) e03107

Contents lists available at ScienceDirect

Heliyon

journal homepage: www.cell.com/heliyon

Research article

An anthropometric evaluation of the scapula, with emphasis on the coracoid process and glenoid fossa in a South African population

R. Khan [a], K.S. Satyapal [a], L. Lazarus [a,*], N. Naidoo [b]

[a] Department of Clinical Anatomy, School of Laboratory Medicine and Medical Sciences, University of Kwa-Zulu Natal, Durban, South Africa
[b] Department of Basic Medical Sciences, College of Medicine, Mohammed Bin Rashid University of Medicine and Health Sciences, Dubai, United Arab Emirates

ARTICLE INFO

Keywords:
Anatomy
Surgery
Glenohumeral joint
Glenoid fossa
Shape
Anthropometric parameters
Coracoid process

ABSTRACT

The exact dimensions of the scapula, including the coracoid process and glenoid fossa, are fundamental in the patho-mechanics of the glenohumeral joint (GHJ); as these structures act as initiators of shoulder movement. The aim of the study was to evaluate the anthropometric parameters of the GHJ, with emphasis on the coracoid process and glenoid fossa. The morphometric (Linear Tools 2012, 0–150mm, LIN 86500963) and morphological parameters of a total of one hundred and sixty-four (n = 164) dry bone scapulae [Right (R): 80; Left (L): 84, Male (M): 68; Female (F): 96] were recorded. *Results*: (i) Shape of glenoid fossa: Type 1: (R) 16.5%, (L) 11.0%; Male (M) 20.1%, Female (F) 7.3%; Type 2: (R) 14.0%, (L) 15.2%; (M) 18.3%, (F) 11.0%; Type 3: (R) 18.3%, (L) 25.0%; (M) 27.4%, (F) 15.9%. (ii) Notch type: Type 1: (R) 1.7%, (L) 7.3%; (M) 6.7%, (F) 2.4%; Type 2: (R) 47.0%, (L) 43.9%; (M) 59.2%, (F) 31.7%. (iii) Vertical diameter of glenoid fossa (VD) (mm): (R) 35.2 ± 3.1, (L) 34.9 ± 3.0; (M) 35.3 ± 3.2, (F) 34.6 ± 2.8. (iv) Horizontal diameter 1 (HD1) of glenoid fossa (mm): (R) 18.4 ± 3.3, (L) 17.5 ± 2.9; (M) 18.2 ± 3.3, (F) 17.4 ± 2.6. (v) Horizontal diameter 2 (HD2) of glenoid fossa (mm): (R) 24.5 ± 2.9, (L) 23.6 ± 2.6; (M) 24.2 ± 2.7, (F) 23.7 ± 2.8. (vi) Length of coracoid process (CL) (mm): (R) 41.7 ± 4.7, (L) 41.5 ± 4.9; (M) 42.1 ± 4.7, (F) 40.7 ± 4.8. (vii) Width of coracoid process (CW) (mm): (R) 13.3 ± 1.9, (L) 14.2 ± 11.9; (M) 13.1 ± 1.9, (F) 15.1 ± 14.5. (viii) Coracoglenoid distance (CGD) (mm): (R) 27.4 ± 8.3, (L) 28.2 ± 3.5; (M) 28.2 ± 7.4, (F) 27.0 ± 3.4. In the present study, Type 3 (oval) was observed to be the predominant glenoid fossa shape with a higher incidence in male individuals and on the right side. Although only notch Types 1 (without a notch) and 2 (with one notch) were observed in this study, Type 2 (one notch) was the most prevalent, presenting with a significant p-value (p = 0.019), suggesting that notch Type 1 (without a notch) and 2 (with one notch) are common findings in the right and left side of individuals. The findings observed in this study may provide knowledge regarding the role of the coracoid parameters in etiology of subcoracoid impingement while knowledge on the glenoid fossa parameters and variations are essential for evaluation in shoulder arthroplasty for glenoid fractures and anterior dislocations, and for glenoid prosthesis designs for the South African population.

1. Introduction

With approximately 2% of the world's population presenting with varying degrees of shoulder instability, pathology of the shoulder is currently considered to be the third most common cause of musculoskeletal diseases in society (Matthews et al., 2006; Lynch et al., 2013). Variations in the coracoid process and glenoid fossa are fundamental to understand rotator cuff disease, glenohumeral osteoarthritis, subcoracoid impingement and shoulder dislocation (Coskun et al., 2006).

The shoulder joint, also known as the glenohumeral joint (GHJ), is an articulation between the spheroidal head of the humerus and the glenoid fossa of the scapula, making the GHJ the most mobile joint in the human body (Standring, 2016). While both articulating surfaces are covered with hyaline cartilage, the humeral head is much larger in relation to the glenoid fossa thereby creating inherent joint instability which may lead to impingement and subluxation (Provencher *et* al., 2009; Standring, 2016). The coracoid process, an osseous structure which projects forward and curves laterally, arises from the superior border of the head of the scapula (Standring, 2016). Muscles that originate from or are inserted into the coracoid process include the short head of biceps brachii, coracobrachialis and pectoralis minor, with four ligaments attaching to this process, viz. coracoclavicular ligament, superior transverse scapular

* Corresponding author.
E-mail address: ramsaroopl@ukzn.ac.za (L. Lazarus).

https://doi.org/10.1016/j.heliyon.2019.e03107
Received 10 April 2019; Received in revised form 29 May 2019; Accepted 19 December 2019

ligament, coracohumeral ligament and coracoacromial ligament (Standring, 2016). In an Italian study conducted by Gumina et al. (1999), the coracoid process exhibited differences in shape, length and direction (Kavita et al., 2013). Since the coracoid process serves as a critical anchor for many tendinous and ligamentous attachments, morphometry that varies from standard reference data may serve as a determinant of sub-coracoid impingement and may allow for early identification, thus preventing progression to a chronic disease (Fathi et al., 2017). The glenoid cavity, a shallow articular surface which is located on the lateral angle of the scapula, functions as the shallow socket of the GHJ by articulating with the head of the humerus (Provencher *et* al., 2009; Standring, 2016). It is characterized as a pear-shaped fossa, with a wider inferior half, the size and shape of which vary greatly (Standring, 2016). Studies have documented glenoid morphology and morphometry to provide literature on the glenoid fossa to aid in the stability of the GHJ (Coskun et al., 2006; Kavita et al., 2013; Mahto and Omar, 2015).

The morphology and morphometry of the glenoid fossa demands attention in shoulder arthroplasty for the treatment of glenoid fractures and in prosthetics for glenoid design and reconstruction (Rajan and Kumar, 2016). Knowledge on the coracoid process may also aid with post-operative treatment of coracoplasty in efforts to improve the road to recovery. As the increase in prevalence of degenerative shoulder disease demands more focus, the provision of accurate and reliable diagnostic data with demographic relevance, may be beneficial to the healthcare system due to the apparent lack of shoulder-related literature in South Africa. Therefore, the aim of this study was to evaluate the anthropometric parameters of the scapula, with emphasis on the coracoid process and glenoid fossa.

2. Material and methods

2.1. General

Dry bone scapulae specimens were obtained from the existing bone bank at the Discipline of Clinical Anatomy, School of Laboratory Medicine and Medical Sciences, University of KwaZulu-Natal. The study was conducted under the auspices of the institutional ethical clearance review committee (Ethical Clearance Number: (BE308/18). All images were captured with the use of a smartphone main camera (Huawei CUN-L22).

2.1.1. Sample series

The study sample was comprised of one hundred and sixty-four (n = 164; Right: 80; Left: 84, Male: 68; Female: 96) unpaired dry bone scapulae (Ages: 18–65 years). The specimens came from a number of ethnic groups (White: 99, Black: 46, Coloured: 14, Indian: 5).

2.1.2. Inclusion and exclusion criteria

Dry bone scapulae displaying evidence of previous damage were excluded. All dry bone scapulae with no previous damage were included.

2.1.3. Statistical analysis

The parameters of the dry bone scapula were measured three times each with a digital caliper by one observer (Linear Tools 2012, 0–150mm, LIN 86500963). The statistical analysis was performed using IBM SPSS, version 25 (Copyright IBM corporation 1989, 2017, Chicago, Illinois, USA). A p-value of less than 0.05 was considered to be statistically significant. The mean values with standard deviations were calculated from the three measurements recorded for each parameter of the scapulae. Intra observer reliability was determined using the multivariate analysis test of the general linear model (Table 4). In cases where frequencies were applied, the weighted mean was calculated using the formula: $\frac{\sum nx}{n}$, where n = sample number and x = incidence within the sample population.

2.2. Methodology

The following morphometric parameters of the scapula were investigated in accordance with the proposed descriptions of Mamatha et al. (2011) and Kavita et al. (2013):

a) *Length of the coracoid process* (mm) (ab): Measured from the tip of the coracoid process to the anterior end of the scapular notch at the superior scapular border (Figure 1a)
b) *Width of the coracoid process* (mm) (cd): Antero-posterior distance measured 1cm posterior to the tip of the coracoid process (Figure 1a)
c) *Coracoglenoid distance* (mm) (ef): distance measured from the anterior rim of the glenoid fossa to the tip of the coracoid process (Figure 1b)
d) *Vertical diameter (VD) of glenoid fossa* (mm) (AB): Maximum distance measured from the inferior point on the glenoid margin to the most prominent part of the supraglenoid tubercle (Figure 2).
e) *Horizontal diameter 1 (HD1) of glenoid fossa* (mm) (EF): Antero-posterior diameter of the superior half of the glenoid fossa, situated mid-point between the superior rim and the mid-point on the vertical diameter (Figure 2).
f) *Horizontal diameter 2 (HD2) of glenoid fossa* (mm) (CD): Maximum breadth of the articular margins of the glenoid fossa, just perpendicular to the vertical diameter (Figure 2)

In addition, morphological observations regarding the shape and notch type of the glenoid fossa were documented.

g) *Shape of the glenoid fossa*: The classification scheme proposed by Mamatha et al. (2011) was adopted and fossae were categorized as: Type 1 (inverted comma-shaped), Type 2 (pear-shaped) or Type 3 (oval-shaped)
h) *Glenoid Notch Type*: The notch type classification scheme proposed by Coskun et al. (2006) was utilized in this study as follows: Type 1 (glenoid fossa without a glenoid notch); Type 2 (glenoid fossa with a pronounced glenoid notch) and Type 3 (glenoid fossa with double glenoid notches).

3. Results

3.1. Intra observer reliability

The mean parameters of CL, CW, CGD, VD, HD1 and HD2 did not yield any statistically significant differences, thus indicating optimum intra-observer reliability of the respective values as similar readings were recorded for all these parameters (Table 1).

3.2. Morphology of the glenoid fossa

3.2.1. Gender

Three shapes of the glenoid fossa were identified in this study, viz. Type 1 (inverted comma shaped), Type 2 (pear shaped) and Type 3 (oval shaped) (Table 2, Figure 3). Only two notch types were identified in this study, viz. Type 1 (without a notch) and Type 2 (one notch) (Table 2, Figure 3).

3.2.2. Laterality

Both right and left sides displayed three glenoid shapes: Type 1 (inverted comma shaped, Type 2 (pear shaped) and Type 3 (oval shaped) (Table 2, Figure 3). Only two notch types were identified in this study, viz. Type 1 (without a notch) and Type 2 (with one notch). A p-value of 0.019 was recorded between notch types on the right and left sides (Table 2, Figure 3).

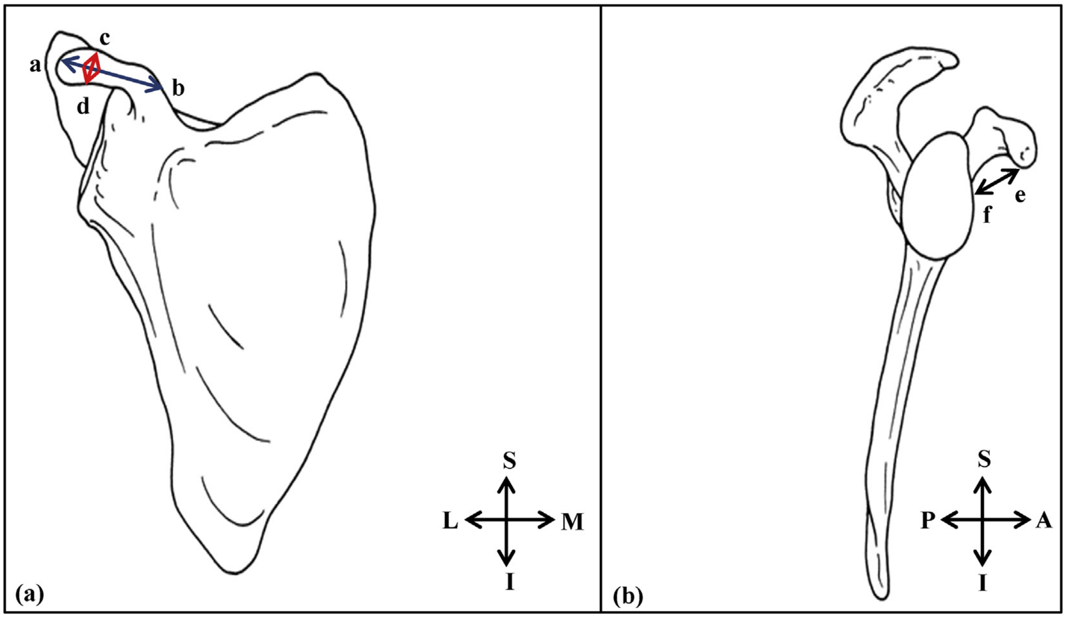

Figure 1. Right scapula displaying morphometric parameters of coracoid process (a) coracoid length and coracoid width (b) coracoglenoid distance. **Key: A**- anterior; **ab-** length of coracoid; **b**- anterior end of suprascapular border; **c**- anterior tip of coracoid process; **cd-** width of coracoid process; **d-** posterior tip of coracoid process; **e-** tip of coracoid process; **ef-** coracoglenoid distance; **f-** anterior rim of glenoid fossa; **I**- inferior; **L**- lateral; **M**- medial; **P**- posterior; **S**- superior.

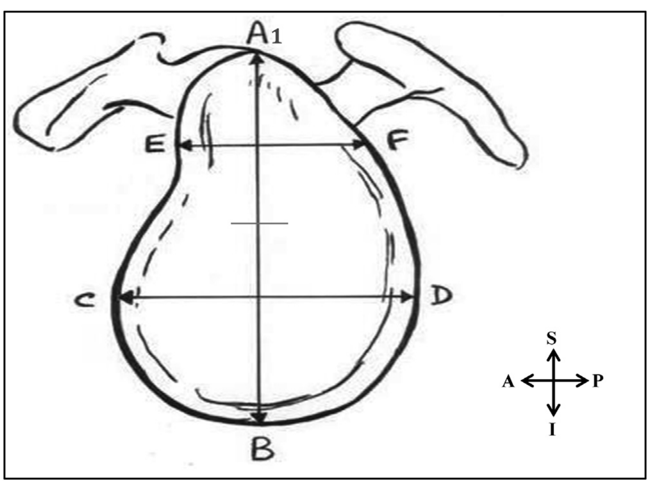

Figure 2. Lateral view of glenoid fossa outlining the vertical (AB) and two horizontal diameters (EF & CD) (Adapted from Mamatha et al., 2011). **Key**: **A-** anterior; **A1-** supraglenoid tubercle of glenoid fossa; **AB-** vertical diameter of glenoid fossa; **B-** inferior rim of glenoid fossa**; C-** anterior articular margin**; CD-** horizontal diameter 2 of glenoid fossa**; D-** posterior articular margin**; E-** anterior rim of upper half of glenoid fossa**; EF-** horizontal diameter 1 of glenoid fossa; **F-** posterior rim of upper half of glenoid fossa; **I**- inferior; **P**- posterior; **S**- superior.

3.3. Morphometry of glenoid fossa and coracoid process

The glenoid fossa and coracoid process parameters together with the coracoglenoid distance is shown in Table 2.

4. Discussion

Degenerative diseases and glenohumeral instability are the leading causes of shoulder pain in the elderly, athletes and young adults (Sahni and Narang, 2014). Both the morphology and morphometry of the coracoid process have been studied previously as these are key elements that provide potential intervention in shoulder pathology and surgery (Verma et al., 2017).

Both glenoid notch types (Type 1 and Type 2) were found to be predominant in males with no reported incidence of Type 3 (double notch) (Figure 3). The variation in glenoid notch types serves as a predisposing factor in anterior dislocation of the GHJ as it has been observed that the glenoid labrum is not attached to the glenoid rim at the site of a notch (Coskun et al., 2006). It has been reported that variation in the pear shape and double notch type of the glenoid fossa are indicative of adaptive changes due to the presence of a vertical axis being created when the arm is elevated (Aiello and Dean, 1990). This vertical axis allows for the head of the humerus to slide into the small upper part of the glenoid fossa, resulting in the variation of shape and notch types that exist in it (Aiello and Dean, 1990). However, this study did not observe Type 3 (with double notches).

The glenoid fossa notch type was previously classified by Coskun et al. (2006). In this study, Type 2 (one notch) was observed in this study as the most prevalent type on both the right and left sides. Although this finding revealed no similarity to the study of Coskun et al. (2006) and Hassanein (2015), the comparison of notch types between the right and left sides yielded a statistically significant p-value ($p = 0.008$). Studies have identified the coracoid process and the glenoid fossa as predisposing factors in anterior dislocation of the joint (Bueno et al., 2012; Kavita et al., 2013).

All three shapes of the glenoid fossa were found to be most prevalent in male individuals (Figure 3). In this study, the shape of the glenoid fossa was categorized according to the classification scheme proposed by Mamatha et al. (2011). Type 3 (oval) was the predominant glenoid shape on both right and left sides, which further corroborated the findings of Mamatha et al. (2011) and Gupta et al. (2015), respectively. An oval-shaped glenoid fossa is suggested to be the most stable glenoid fossa shape with the glenoid labrum being attached along all borders of the glenoid fossa (Coskun et al., 2006). On the contrary, Type 2 (pear) was the least prevalent shape on the right side, which differed from higher prevalence reported in previous studies (Dhinsda and Singh, 2014; Chhabra et al., 2015; Mamatha et al., 2011) (Table 3). The pear-shaped glenoid fossa is considered to be more vulnerable to shoulder dislocation as the glenoid labrum is not attached to the posterior glenoid fossa (Coskun et al., 2006). Type 1 (inverted comma) was seen to be the least prevalent shape on the left side in this study and revealed a lower prevalence than that of the reviewed literature (Dhinsda and Singh,

Table 1. Intra observer reliability.

Descriptive Statistics			Multivariate Analysis: Effect			
Parameter	Dataset	Mean ± Std. Deviation (mm)	Pillai's Trace	Wilk's Lambda	Hotelling's Trace	Roy's Largest Root
CL	1	41.0 ± 1.5	0.017	0.983	0.017	0.017
	2	41.6 ± 4.8				
	3	41.0 ± 1.5				
CW	1	13.7 ± 8.9	0.001	0.999	0.001	0.001
	2	13.7 ± 8.6				
	3	13.6 ± 8.9				
CGD	1	27.8 ± 6.3	0.001	0.999	0.001	0.001
	2	27.8 ± 6.3				
	3	28.0 ± 6.4				
VD	1	34.6 ± 1.5	0.023	0.978	0.023	0.023
	2	35.1 ± 3.1				
	3	35.0 ± 3.1				
HD1	1	18.0 ± 3.1	0.000	1.000	0.000	0.000
	2	18.0 ± 3.2				
	3	18.0 ± 3.2				
HD2	1	24.0 ± 2.8	0.996	0.004	0.996	0.996
	2	24.1 ± 2.8				
	3	23.5 ± 2.7				

Key: CL: coracoid length; CW: coracoid width; CGD: coracoglenoid distance; VD: vertical diameter; HD1: horizontal diameter 1; HD2: horizontal diameter 2.

Table 2. Morphological parameters of the coracoid process.

Parameters		Morphology (%) of the Glenoid Fossa					
		Notch Type			Shape		
		1 (without a notch)	2 (one notch)	3 (double notch)	1 (inverted comma)	2 (pear)	3 (oval)
Laterality	Right (n = 80)	1.7	47.0	0	16.5	14.0	18.3
	Left (n = 84)	7.3	44.0	0	11.0	15.2	25.0
p-value		0.019*			0.068		
Gender	Male (n = 68)	6.7	59.2	0	20.1	18.3	27.4
	Female (n = 96)	2.4	31.7	0	7.3	11.0	15.9
p-value		0.525			0.310		

* Significant p-value.

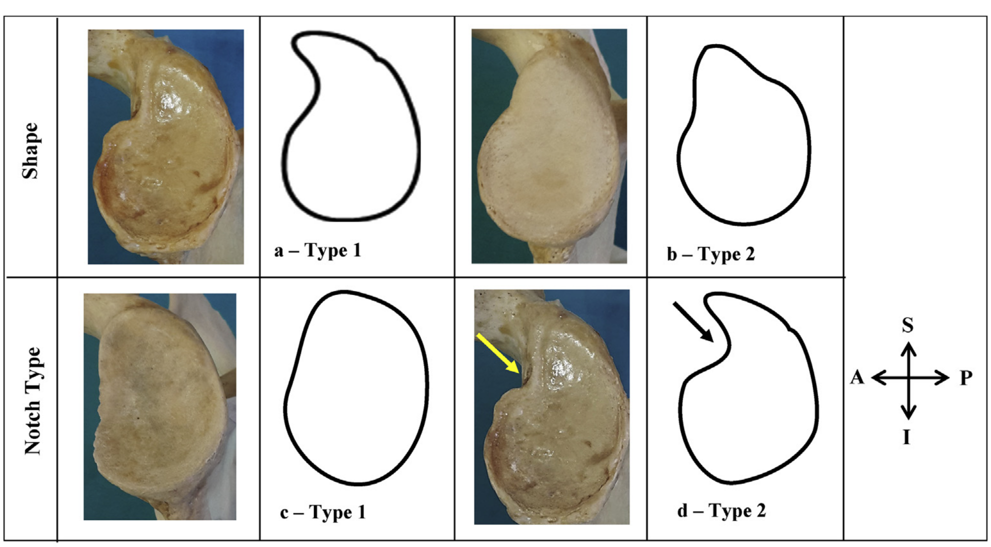

Key: **A**- anterior; **I**- inferior; **P**- posterior; **S**- superior

Figure 3. Morphology of the glenoid fossa. Shape: (a)- Type 1 (inverted comma); (b)- Type 2 (pear); Notch: (c)- Type 1 (without a notch); (d)- Type 2 (with one notch). **Key**: **A**- anterior; **I**- inferior; **P**- posterior; **S**- superior.

Table 3. Morphometric parameters of the coracoid process and glenoid fossa.

Parameters		Glenoid Fossa Morphometry (mm)			Coracoid Process Morphometry (mm)		
		VD	HD1	HD2	CL	CW	CGD
Laterality	Right (n = 80)	35.2 ± 3.1	18.4 ± 3.3	24.5 ± 2.9	41.7 ± 4.7	13.3 ± 1.9	27.4 ± 8.3
	Left (n = 84)	34.9 ± 3.0	17.5 ± 2.9	23.6 ± 2.6	41.5 ± 4.9	14.2 ± 11.9	28.2 ± 3.5
p-value		0.471	0.063	0.064	0.756	0.499	0.453
Gender	Male (n = 68)	35.3 ± 3.1	18.2 ± 3.3	24.2 ± 2.7	42.1 ± 4.7	13.1 ± 1.9	28.2 ± 7.4
	Female (n = 96)	34.6 ± 2.8	17.4 ± 2.6	23.7 ± 2.8	40.7 ± 4.8	15.1 ± 14.5	27.0 ± 3.4
p-value		0.214	0.092	0.240	0.091	0.155	0.253

Key: VD: vertical diameter, HD1: horizontal diameter 1; HD2: horizontal diameter 2; CL: coracoid length; CW: coracoid width.
CGD: coracoglenoid distance.

Table 4. Incidence of the shape of the glenoid fossa as reported in earlier studies.

Author (year)	Sample size (n)	Incidence (%) (x)					
		Type 1 (Inverted comma shaped)		Type 2 (Pear shaped)		Type 3 (Oval shaped)	
		Right (%)	Left (%)	Right (%)	Left (%)	Right (%)	Left (%)
Dhinsda and Singh (2014)	80	29.3	35.9	48.8	46.2	22.0	17.9
Chhabra et al. (2015)	126	12.7	21.8	54.9	47.3	32.4	30.9
El-Din and Ali (2015)	160	<u>16.3</u>	20.0	35.0	28.0	48.8	53.0
Gupta et al. (2015)	60	40.0	36.7	43.3	40.0	<u>16.7</u>	23.3
Hassanein (2015)	68	31.6	30.0	44.7	46.7	23.7	23.3
Mamatha et al. (2011)	202	34.0	33.0	46.0	43.0	20.0	<u>24.0</u>
Weighted Mean		25.8	28.3	45.1	40.7	29.2	31.0
This Study (2018)	164	<u>16.5</u>	11.0	14.0	15.2	<u>18.3</u>	<u>25.0</u>

*underlined text shows similarities of current studies with previous studies.

2014; Gupta et al., 2015; Hassanein, 2015; Mamatha et al., 2011). In inverted comma-shaped glenoid fossa, the glenoid labrum is not rigidly attached to the glenoid margin. During arthroscopy, this structure predisposes the GHJ to a labral tear, Buford complex or sublabral foramen (Tuite et al., 2001; Alashkham et al., 2017).

In the current study, incidences recorded for all three shapes of the glenoid fossa on both right and left sides were distinctively lower than the weighted means deduced from previous studies (Table 4). Mamatha et al. (2011) was likely to offset the weighted mean values due to the larger sample size (n = 202). Therefore, the study by Mamatha et al. (2011) contributed a higher sample number to the calculation of the weighted mean and possibly resulted in an over-estimation of the values.

The mean VD, HD1, HD2, CL and CGD were observed to be larger in males while females presented with a larger mean CW and this finding may provide specific information on the male and female population in South Africa as it may aid clinicians in gender-based information for the treatment of shoulder pathologies and prosthetic designs. The mean VD in this study was found to be larger on the right side. This confirmed the findings of This confirmed the findings of Dhinsda and Singh (2014), Mahto and Omar (2015), Gupta et al. (2015) and Hassanein (2015). Although HD1 has only been investigated in a limited number of studies, the values of the current study were similar to the studies conducted by Mamatha et al. (2011) and Chhabra et al. (2015), where the mean HD1 was found to be larger on the right side (Table 4). The mean HD2 was also observed to be larger on the right side, agreeing with the reports of previous studies (Mamatha et al., 2011; Gupta et al., 2015; Hassanein, 2015; Mahto and Omar, 2015) (Table 4).

Complications in prosthetic design, sizing and positioning in total shoulder arthroplasty arises from anatomical variations which increases the likelihood of failure for full GHJ congruency, therefore, knowledge on the normal and variational anatomy of the scapula is imperative during shoulder arthroscopy to avoid such complications (Churchill *et* al., 2001; Monk et al., 2001; Coskun et al., 2006). Glenoid loosening is considered the most common indication for a shoulder surgery revision and in order to avoid this, successful total shoulder replacement requires a matched fit between the underlying bone and the glenoid component (McMurray et al., 2012; Owaydhah et al., 2017).

The coracoid process is a hook-shaped bone structure projecting antero-laterally from the superior aspect of the scapular neck (Mohammed et al., 2016). The coracoid process, aptly defined by Matsen et al. (1990) as the "lighthouse of the shoulder", is a reference landmark in arthroscopy for access into the shoulder (Mercer et al., 2011). The coracoid process serves as an important anchor for several tendinous and ligamentous structures including the pectoralis minor tendon, coracobrachialis, short head of the biceps brachii muscle, the coracohumeral, coracoacromial, coracoclavicular and suprascapular ligaments (Mohammed et al., 2016).

Individuals showed larger mean CL on the right side in the present study. This finding compared favorably and concurred with the studies conducted by Fathi et al. (2017) and Verma et al. (2017). However, it differed from the reports of Coskun et al. (2006) and Kavita et al. (2013) where the mean CL was relatively decreased (Table 3). Individuals on the left side showed a larger mean CW and compared favorably with the study by Coskun et al. (2006), whereas the study by Fathi et al. (2017) and Verma et al. (2017) showed much smaller mean CWs as compared to the present study (Table 4). The mean CGD was increased on the left side and differed with the study by Kavita et al. (2013), where CGD was reported to be larger on the right side (Table 4).

One of the fundamental principles of shoulder surgery is an approach which is lateral to the coracoid process to avoid vital neurovascular structures which run medially to the coracoid process (Alobaidy and Soames, 2016; Mohammed et al., 2016). The open procedure which transfers the coracoid process to the glenoid fossa and enhances the GHJ stability is known as the Latarjet and Bristow-Helfet procedure. The Bristow-Helfet project places the larger axis of the graft to the glenoid fossa while the in the Latarjet procedure, the larger axis of the graft is places parallel to the glenoid fossa (Pereira and Gutierres, 2017). These procedures have been reported with surgical complications where precise techniques and an understanding of the GHJ anatomy will reduce the complications of shoulder surgery (Griesser et al., 2013). Therefore, to ensure that a safe approach is maintained, the morphometry of the coracoid process is imperative (Mohammed et al., 2016).

The weighted means could suggest that the present study provides a more accurate means of determining the values. The presence of unequal right and left sides (R = 80, L = 84) could account for the difference in prevalence of the present study with the weighted mean as this is not a bilateral representation. The current study may be improved in the future by investigating bilateral scapulae of the same individual, thus providing more reliable results. It is recommended that inter-observer reliability indices are incorporated to further reduce standard errors in measurement and observation. Investigation of the coracoid process and glenoid fossa should also be conducted on imaging resources as these diagnostic tools would prove beneficial in clinical practice.

5. Conclusion

In the present study, Type 3 (oval) was observed to be the predominant glenoid fossa shape with a higher incidence in male individuals and on the right side. Although only notch Types 1 (without a notch) and 2 (with one notch) were observed in this study, Type 2 (one notch) was the most prevalent, presenting with a significant p-value ($p = 0.019$), suggesting that notch Type 1 (without a notch) and 2 (with one notch) are common findings in the right and left side of individuals. Updated anatomical knowledge regarding the variation of the bony glenoid fossa and coracoid process may present as a pre-requisite for the successful management of shoulder surgery in coracoplasty and in glenoid prosthesis designs for the South African population by taking into account gender and laterality-based data.

Declarations

Author contribution statement

R. Khan: conceived and designed the experiments; performed the experiments; analyzed and interpreted the data; contributed reagents, materials, analysis tools or data; wrote the paper.

L. Lazarus, KS. Satyapal: conceived and designed the experiments; wrote the paper.

N. Naidoo: conceived and designed the experiments; analyzed and interpreted the data; wrote the paper.

Funding statement

This research did not receive any specific grant from funding agencies in the public, commercial, or not-for-profit sectors.

Competing interest statement

The authors declare no conflict of interest.

Additional information

No additional information is available for this paper.

References

Aiello, L., Dean, C., 1990. An Introduction to Human Evolutionary Anatomy. Academic Press, London.
Alashkham, A., Alraddadi, A., Soames, R., 2017. The glenoid notch and its clinical implications. Revista Argentina de Anatomia Clinica 9 (1), 11–17.
Alobaidy, M.A., Soames, R.W., 2016. Evaluation of the coracoid and coracoacromial arch geometry on Thiel-embalmed cadavers using the three-dimensional MicroScribe digitizer. J. Shoulder Elb. Surg. 25 (1), 136–141.
Bueno, R.S., Ikemoto, R.Y., Nasamento, L.G.P., et al., 2012. Correlation of coracoid thickness and glenoid width. Am. J. Sports Med. 40 (7), 1664–1667.
Coskun, N., Karaali, K., Cevikol, C., et al., 2006. Anatomical basis and variation of the scapula in Turkish adults. Saudi Med. J. 27 (9), 1320–1325.
Chhabra, N., Prakash, S., Mishra, B.K., 2015. An anatomical study of glenoid cavity: its importance in shoulder prosthesis. Int. J. Anat. Res. 3 (3), 1419–1424.
Churchill, R.S., Brems, J.J., Kotschi, H., 2001. Glenoid size, inclination and version: an anatomic study. J. Shoulder Elb. Surg. 10 (4), 327–332.
Dhinsda, G.S., Singh, Z., 2014. A study of morphology of the glenoid cavity. J. Evol. Med. Dent. Sci. 3 (25), 7036–7043.
El-Din, N.W., Ali, M.H.M., 2015. The pattern of the acromion and glenoid cavity in Egyptian scapulae. J. Clin. Diagn. Res. 9 (8), AC08–AC11.
Fathi, M., Cheah, P.S., Ahmad, U., et al., 2017. Anatomic variation in morphometry of human coracoid process among Asian population. BioMed Res. Int. 1–10.
Griesser, M.J., Harris, J.D., McCoy, B.W., Hussain, W.M., Jones, M.H., Bishop, J.Y., Miniaci, A., 2013. Complications and re-operations after Bristow-Latarjet shoulder stabilization: a systematic review. J. Shoulder Elb. Surg. 22 (2), 286–292.
Gumina, S., Postacchini, F., Orsina, L., Cinotti, G., 1999. The morphometry of the coracoid process-its aetiological role in subcoracoid impingement. Int. Orthop. 23 (4), 198–201.
Gupta, S., Magotra, R., Kour, M., 2015. Morphometric analysis of glenoid fossa of scapula. J. Evol. Med. Dent. Sci. 4 (45), 7761–7766.
Hassanein, G.H.E., 2015. Morphometry of the glenoid fossa in adult Egyptian scapula. Int. J. Appl. Res. 3 (2), 1138–1142.
Kavita, P., Singh, J., Geeta, et al., 2013. Morphology of coracoid process and glenoid cavity in adult human scapulae. Int. J. Anal. Pharm. Biomed. Sci. 2 (2), 62–65.
Lynch, E., Lombard, A.J.J., Coopoo, Y., et al., 2013. Shoulder injury incidence and severity through identification of risk factors in rugby union players. Pak. J. Med. Sci. 29 (6), 1400–1405.
Mahto, A.K., Omar, S., 2015. Dimensions of glenoid fossa of scapula: implications in the biomechanics of an implant design. Int. J. Sci. Study 3 (4), 146–148.
Mamatha, T., Pai, S.R., Murlimanju, B.V., et al., 2011. Morphometry of glenoid cavity. J. Allied Health 10 (3), 7.
Matsen, F.A., Thomas, S.C., Rockwood, C.A., 1990. Anterior glenohumeral instability. In: Rockwood, C.A., Matsen, F.A. (Eds.), The Shoulder. WB Saunders, Philadelphia, pp. 336–367.
Matthews, T.J., Hand, G.C., Rees, J.L., 2006. Pathology of the torn rotator cuff tendon. J. Bone Joint. Surg. Br. 74, 151–153.
McMurray, D., Monk, A.P., Limb, D., 2012. The classification of glenoid version and its relevance to shoulder stability. Shoulder Elb. 4 (3), 158–162.
Mercer, D., Saltzman, M., Neradilek, M.B., et al., 2011. A reproducible and practical method for documenting the position of the humeral head center relative to the scapula on standardized plain radiographs. J. Shoulder Elb. Surg. 20, 363–371.
Mohammed, H., Skalski, M.R., Patel, D.B., Tomasian, A., Schein, A.J., White, E.A., Hatch, G.F., Matcuk, G.R., 2016. Coracoid process: the lighthouse of the shoulder. RadioGraphics 36, 2084–2101.
Monk, A.P., Berry, E., Limb, D., Soames, R.W., 2001. Laser morphometric analysis of the glenoid fossa of the scapula. Clin. Anat. 14 (5), 320–323.
Owaydhah, W.H., Alobaidy, M.A., Alraddadi, A.S., Soames, R.W., 2017. Three-dimensional analysis of the proximal humeral and glenoid geometry using MicroScribe 3D digitizer. Surg. Radiol. Anat. 39 (7), 767–772.
Pereira, A., Gutierres, M., 2017. Complications of coracoid transfer procedures for the treatment of recurrent shoulder dislocation. Porto BioMed. J.
Provencher, M.T., McNickle, A., L'Heureux, D.R., et al., 2009. Post-surgical glenohumeral arthritis in young adults. Athroscopy 25, 37–38.
Rajan, Y.S., Kumar, S.K.S., 2016. Morphometric study on bicipital groove among South Indian population. J. Clin. Diagn. Res. 10 (7), AC01–AC03.
Sahni, Narang, 2014. Recent advances in shoulder surgery. J. Orthop. Allied Sci. 39 (1), 14–23.
Standring, S., 2016. Gray's Anatomy: the Anatomical Basis of Clinical Practice, fourth ed. Elsevier Limited.
Tuite, M.J., Blankenbaker, D.G., Seifert, M., Ziegert, A.J., Orwin, J.F., 2001. Sublabral foramen and Buford complex: inferior extent of the unattached or absent labrum in 50 patients. Radiology 223 (1), 137–142.
Verma, U., Singroha, R., Malik, P., et al., 2017. A study on morphometry of coracoid process of scapula in north Indian population. J. Res. Med. Sci. 5 (11), 4970–4974.